AERODYNAMIC OPTIMIZATION OF SUPERSONIC TRANSPORT CONFIGURATIONS

M. Orlowski, U. Herrmann
DLR, Institute of Design Aerodynamics
Lilienthalplatz 7, D-38108 Braunschweig, Fed. Rep. of Germany

1.Abstract

In the present paper first steps towards the aerodynamic optimization of supersonic civil transport configurations are described. The DLR optimization tool MODeM is introduced. Optimization capabilities are demonstrated using an unconventional waverider-like generic SCT configuration. Furthermore sensitivities of the lift to drag ratio with respect to five fuselage design variables of conventional wing/body configurations are studied.

2.Introduction

Analysis of future air traffic has renewed interest in supersonic civil transport (SCT). A new generation of supersonic aircraft requires essential improvements over Concorde and TU 144 in aerodynamic performance, engine efficiency, pollution and noise in order to ensure economic viability and to fulfill environmental constraints.

The main improvement in aerodynamic performance relates to the lift to drag ratio. At cruise conditions a configuration with prescribed volume and minimal drag has to be achieved. Noise aspects demand subsonic cruise over populated areas. Therefore, future SCTs will be dual-point designs, i.e. drag has to be minimal at supersonic and transonic cruise conditions. Current and expected FAR noise constraints at take off and landing influence the design. Necessary noise reduction at take off and landing requires additional drag reduction. It is believed that attached flow is necessary to prevent vortices and their accociated drag. On the contrary this reduces the attainable lift. The aircraft's planform area has to be increased to compensate for this. A greater planform influences aerodynamic performance also at sub- and supersonic cruise conditions. Designing an aircraft using conventional approaches of inverse methods demands knowledge of pressure distributions to obtain a shape with minimal drag and good aerodynamic performance. Especially a design with good performance at more than one cruise condition seems to be extremly difficult using the inverse design approach. It is not clear how geometric constraints could be represented directly in pressure distributions.

A different approach is based on controlled shape variations of the aircraft in general or parts of the aircraft. In this class of methods an analysis code is coupled with a numerical optimizer to judge aerodynamic effects of the aircraft's changing shape. The optimizer determines the shape variation of a given datum aircraft based on results of previous attempts and given constraints. It finally establishes the variation that designs a better aircraft shape for given requirements and constraints. The absolut best aircraft shape for identical boundary conditions is found if the absolut maximum of the (constraint) design variable space is found.

DLR is working on such an optimization tool using controlled variations, called Multi-point Optimization Design Method (MODeM). It couples CFD and optimization methods based on previous experience with super- and hypersonic configurations [1] and the optimization of transonic airfoils and wings [2]. Attention is payed to enable the tool to treat unconventional configurations such as waveriders and oblique flying wings as well as conventional wing-body configurations. In the present work first steps towards this optimization tool to design a supersonic civil transport with maximum aerodynamic performance are described. It focuses on results gained with preliminary versions of MODeM's moduls.

3.Optimization Tool

The control structure of MODeM is sketched in **Fig. 1**. Prerequisite for any optimization is a geometry representation which allows variations of the geometry with a minimum number of parameters. The implemented geometry generator is based on a set of mathematical functions introduced by Sobieczky [3] and has been extended to be able to treat conventional and unconventional configurations in the same manner. The mesh generation process consists of the generation of the surface mesh, the far-field and the volume mesh. For the investigations to be reported in this paper meshes have been generated with a preliminary mesh generator which is based only on algebraic mesh generation tools [4],[5]. In the final version of MODeM mesh generation will be done by an improved version of the DLR general purpose mesh generation system MegaCads [6].

In general optimization procedures require fast and robust flow solvers. They have to guarantee high accuracy to judge effects of incremental geometry variations even on medium dense meshes in order to minimize computational expense. The DLR flow sol-

ver [7] fulfills these requirements. It solves the Euler- or Navier-Stokes equations in integral form. The method is based on finite volumes. The spatial discretization is an improved version of the AUSM flux vector splitting formulation [8]. The time integration is done by an explicit Runge-Kutta multistage scheme. Convergence to steady state can be improved by using multiple grids or acceleration technics like local time stepping and implict residual smoothing. Results presented in this paper are calculations on single meshes.

Most of the CPU-time for an optimization cycle is spent on the flow solver because each geometry variation requires a new flow solution. Therefore, a mathematical optimization algorithm with minimal use of the flow solver is necessary. Finite difference and adjoint equation methods are considered. In a first step a finite difference method using parabolic interpolation is implemented. It is obvious that minimal drag at supersonic and transsonic onflow conditions will require attached flow. Therefore, in order to reduce the numerical effort, only inviscid flows are calculated. Viscous drag is taken into account by a surface area dependend flat plate analogy.

MODeM is entirely steered by a task broker. This approach enables to implement the tool as a collection of independent modules. Thus, maintenance is easy and updates of the modules can be applied at once. As indicated in Fig. 1, the approach enables also to use the inherent parallelity of the problem to speed up the optimization by using several computers to calculate results.

4.Results

Primary task of any SCT aircraft is the transportation of a sufficient large volume of payload. The necessary volume can be obtained by integrating the fuselage into the wing as in **Fig. 2** or by a conventional wing-body configuration. Unconventional, blended configurations are expected to outperform conventional wing-body configurations aerodynamically [1]. All parts of the blended aircraft serve as nearly equally loaded lifting surfaces and therefore generate low levels of drag. Because the volume can be distributed in more spanwise direction than in conventional configurations, their overall length will be reduced compared to classical wing-body configurations. This is favourable for ground handling. Furthermore, it has positive effects on the structural weights and on landing gear design. As mentioned, the geometry generator implemented in MODeM is formulated to treat both types of aircraft configurations. Being able to vary the fuselage from a conventional shape with circular cross sections up to a shape which resembles the highly swept forward portion of delta wings will enable the optimizer to find the best SCT shape regardless whether the optimization procedure starts from a conventional wing-body or from a blended configuration.

This paper will report first steps towards this goal. The functionality of MODeM by optimizing a given configuration is demonstrated. Furthermore, aspects of the necessary numerical accuracy are investigated. Finally design variable sensitivities of wing-body fuselages are shown.

The capabilities of MODeM have first been tested on an unconventional SCT example configuration. Fig. 2 shows the surface and the volume mesh (64x32x82 cells) of a double delta waverider. Onflow Mach number is 2, a typical SCT cruise speed assumption. The lift to drag ratio will be maximized by optimizing first the axial and then the spanwise camber distributions of the configuration's first delta. The angle of attack of the whole configuration is optimized additional in both cases. Due to performance reasons, optimization is carried out on a coarse mesh (32x16x41 cells). **Fig. 3** depicts lift to drag ratios of the initial and both optimized configurations versus angle of attack. The calculated optima agree well with the given polars confirming the resultend values for the angle of attack. Improvements of the lift to drag ratio up to 7% through axial camber optimization and up to 20% through spanwise camber optimization are achieved. The optimization history is given in **Fig. 4**. Spanwise chamber distribution and angle of attack are varied to maximize the lift to drag ratio. Note that the most increase of the inviscid lift to drag ratio is reached within the first 12 steps. **Fig. 5** sketches the resultend cross section of the configuration due to spanwise camber optimization at 40% of the body length.

For conventional wing-body configurations numerical accuracy aspects for fuselage optimization are discussed. Furthermore, sensitivities of the configuration's attainable lift to drag ration due to fuselage design variable variations are investigated. Typical planforms of the range of investigated generic SCT wing-body configuration are shown in **Fig. 6**. The wing geometry is fixed and has a halfspan of 21 meters. Prior to the fuselage investigations the wing profiles and their twist distribution have been optimized [9] for a similar wing planform. Onflow conditions for all investigations are: Mach number 2 and 3 degrees angle of attack.

The fuselage consists of a front cone, a cylindrical part and a rear cone for a given radius. All three parts are variable in length, keeping the required volume for 250 passengers constant. At first a fuselage radius of 1.5m is choosen. The front and rear cone lenghts are varied between 15 and 23 meters. The overall dimensions of the aircraft with this fuselages become: 42m span and a length between 84 to 94 meters.

The used mesh around the generic SCT wing-body configuration is shown in **Fig. 7**. Note the grid clustering towards the intersection of the wing leading and trailing edges with the body. Three different cone length (C=15, 19, 23m) for a fuselage radius of 1.5 meters (R=1.5m) are calculated. Mesh density effects on the prediction accuracy of the calculated aerodynamic coefficients are investigated. This is done by calculating the aerodynamic coefficients of the three fuselages, each on three different dense meshes. In **Fig. 8** the mesh dependence of the aircrafts inviscid drag (left hand side) and the lift to drag ratios (right hand side) are given. The coarse mesh consists of 24x12x26 cells in longitudinal (N_X), bodynormal (N_Y) and circumferential (N_Z) direction. The medium and fine meshes have 48x24x52 and 96x48x104 cells respectively.

For the three fuselages of different length the same inviscid drag change with mesh density is found. Furthermore, the differences between medium and fine mesh are in the order of 3% with respect to the drag prediction and of 0,4% with respect to the lift to drag ratio. This small differences, especially for the most interesting lift to drag ratio, justifies the further exclusive use of the medium dense mesh. The advantage is obvious: reduced numerical effort compared to the fine mesh for all investigations.

The convergence behaviour of the calculated aerodynamic coefficients is investigated additionally. In **Fig. 9** both, lift and drag for the different fuselage lengths are plotted against the residual reduction of the conservation of mass for the medium mesh. **Fig. 10** repeats this plot for the fine mesh. While the calculated drag does not change significantly after two orders magnitude of residual reduction, the lift prediction needs three orders magnitude residual convergence. This holds for both meshes but note that the fine mesh requires more iterations to reach the same level of residuum reduction than the medium mesh. Furthermore, each iteration is more expensive on the fine mesh. To be safe all fuselage design variable sensitivity studies are converged about five orders of magnitude on the medium dense mesh.

The following results show the sensitivities of the lift to drag ratio of the configuration with respect to selected fuselage design variables. As mentioned, the fuselage is assembled out of a front cone, a cylindrical part and a rear cone for a given radius. All three parts are variable in length, keeping the required volume for 250 passengers constant. Five fuselage design variables are choosen to be investigated:

- the fuselage cone length (front and rear cone are of identical length)
- the fuselage incidence angle (relative to the wing and the onflow direction)
- the maximal fuselage width (non circular cross section)
- the relative horizontal position between wing and fuselage
- the relative vertical position between wing and fuselage.

First the lift to drag ratios for different cone lengths C and two fuselage radii (radius of the cylindrical fuselage part) are shown in **Fig. 11**. The selected fuselage radii correspond to 5 and 6 seats per row (R=1.5 m; resp. R=1.75 m). The overall length of the wider fuselage varies from 74 to 83 m (84 to 94 m for the slender body). Utilizable volume inside the cones is taken into account and reduces the necessary length of the cylindrical fuselage part. On the left hand side of Fig. 11 the sum of inviscid and viscous drag (determined from a flat plate's turbulent viscous drag at M= 2; Re= $145*10^6$ and scaled with the aircraft's surface area) is calculated to obtain the viscous lift to drag ratio. The right hand side of this graph gives the pressure drag. The slender fuselage (R=1.5m) generates less pressure drag and reaches the best lift to drag ratio at cone lengths C greater than 25m. The wider fuselage shows a greater sensitivity to the cone length and reaches a flat optimum around 22m cone length. The greater flow turning angle due to the increased fuselage radius raises the pressure drag level compared to the slender body. By increasing the fuselage diameter by 16% (R= 1.5m > R= 1.75m) the sensitivity of the cone length variable doubles but the lift to drag ratio reduces for only ~1% ($C_L/\Sigma C_D$= 9.256 > 9.161). Calculating this small aerodynamic performance differences on relatively coarse meshes requires confidence that aerodynamic effects through geometric variations can be resolved. Mesh inherent discretization errors can never be prevented. But it must be guaranteed that throughout the geometric variation the distribution of the inherent local discretization error stays the same. This is a necessary requirement especially for the use of relatively coarse meshes to be able to compare results of any geometric variations.

In **Fig. 12** the sensitivity of the fuselage incidence angle is investigated. The wider fuselage is choosen having the shorter nearly optimal cone length (C= 21m; overall length: 81m) because the possible range of incidence angle variation is greater than on the slender fuselage. It is found that the sensitivity to this design variable is similar to that of the cone length. Note that the pressure drag changes much more with fuselage incidence angle than with cone length. As expected it increases with inclination. However lift to drag ratios are not decreased. This is

due to increasing lift coefficients with fuselage incidence angle.

The next two sensitivities focus on the relative position between fuselage and wing. The sensitivity of the horizontal (x) position of the wing relative to the fuselage middle position (R= 1.75m; C= 21m) is given in **Fig. 13**. **Fig. 14** depicts the vertical (z) position sensitivity. Negative z positions correspond to a low wing plane. Both sensitivities are less strong than the cone length or the fuselage incidence angle. The tendencies indicate that the aircraft should be a low wing type plane with the wing pushed as far to the front as area ruling indicates.

The lift to drag ratio variations with the fuselage width B are given in **Fig. 15**. The body varies from the slender circular cross section fuselage (R= 1.5m) to a fuselage with a cross section consisting of a rectangular inner part and a half circle on each side with the radius R= 1.5m. The cone lenght is fixed to C= 21m. Overall length varies from 75 to 91m. The weak sensitivity indicates a noncircular fuselage cross section to be preferrable. This holds also compared to the wider circular cross section fuselage (R= 1.75m) which generates a higher level of pressure drag at identical cone length.

5.Conclusion

The structure and main parts of DLR's multi-point optimization design method (MODeM) are described. Optimization of a waveriderlike SCT example configuration with this method is presented first. It is performed through variation of spanwise chamber distribution and angle of attack. The optimization procedure improves the inviscid lift to drag ratio by 20%. After demonstrating the methods optimization capabilities for a blended configuration conventional wing-body configurations are addressed. Sensitivities of the viscous lift to drag ratios with respect to fuselage design variables are studied. Numerical investigations indicate minimal required mesh sizes and necessary convergence levels for this task. Five fuselage design variables are investigated. Starting with fuselages of circular cross sections, cone length and fuselage incidence angle sensitivities are studied. These variables show the strongest influences and change the viscous lift to drag ratio in the order of 3%. Weaker sensitivities (~1%) are found for the relative horizontal and vertical fuselage-wing position and the fuselage width variation. Comparing the demonstrated 20% improvement in aerodynamic efficiency of the waverider with the 3% fuselage sensitivities needs further explanation. One should keep in mind that viscous drag is neglected in the waverider wing case. Consideration of viscous drag would considerably reduce (nearly halfen) the optimization potential found. Furthermore, note that the fuselages pressure and viscous drag is small (about 30%) compared to the wings contribution. Both facts lead to the conclusion that sensitivities of similar magnitude are found for the wing and major fuselage design variables. Interpretation of the sensitivities form this picture of a aerodynamically optimal aircraft. It's fuselage will have a slightly non circular cross section and a cone length of nearly 20m. The aircraft's wing should be placed as far as possible downward and as close as possible towards the body's apex. Depending on what wing and fuselage design variables will be choosen to optimize a whole configuration, it seems probable to obtain a blended configuration as an optimal aircraft.

6.References

[1] Eggers, Th.; Strohmeyer, D.; Nickel, H.; Radespiel, R.:
Aerodynamic Off-Design Behavior of Integrated Waveriders From Take-Off up to Hypersonic Flight.
6th International Aerospace Planes and Hypersonics Technologies Conference, Chattanooga, USA, 1995.

[2] Bartelheimer, W.:
An Improved Integral Equation Method for the Design of Transonic Airfoils and Wings.
13th AIAA Applied Aerodynamics Conference, San Diego, USA, 1995.

[3] Sobieczky, H.; Choudhry, S. I.; Eggers, Th.:
Parameterized Supersonic Transport Configurations.
7th European Aerospace Conference, Toulouse, France, 1994.

[4] Abolhassani, J.S.; Stewart, J.E.:
Surface Grid Generation in a Parameter Space.
J. of Comp. Physics, 113, p. 112-121, 1994.

[5] Herrmann, U.:
IMESH - An Interactive Mesh Generation Package for Graphics Super Workstations.
3rd Int. Conference on Numerical Grid Generation in Computational Fluid Dynamics and related Fields, Barcelona, Spain, 1991.

[6] Brodersen, O.; Hepperle, M.; Ronzheimer, A.; Rossow, C.-C.; Schöning, B.:
The Parametric Grid Generation System MegaCads
5th Int. Conference on Numerical Grid Generation in Computational Field Simulations, p. 353-362, USA, 1996

[7] Kroll, N.; Radespiel, R.; Rossow, C.-C.:
Accurate and Efficient Flow Solvers for 3D Applications on Structured Meshes.
AGARD FDP/VKI Special Course on Parallel Computing in CFD, Brussels, Belgium, 1995.

[8] Kroll, N.; Radespiel, R.:
An Improved Flux Vector Splitting Discretization Scheme for Viscous Flows.
DLR-FB 93-53, 1993.

[9] Doherty, J. J.; Parker, N. T.:
Dual-Point Design of a Supersonic Transport Wing using a Constrained Optimization Method. 7th European Aerospace Conference, Toulouse, France, 1994.

7.Figures

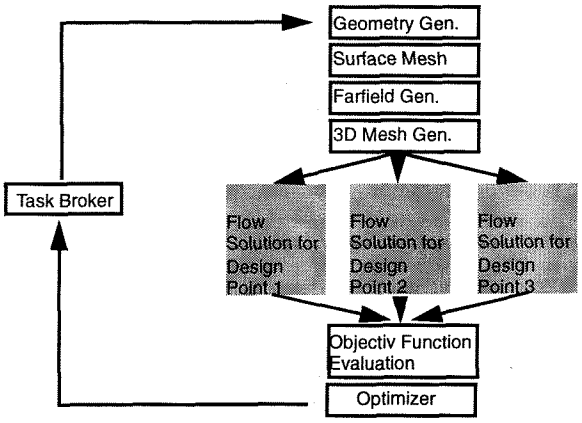

Fig. 1 Control structure of the Multi-point Optimization Design Method (MODeM).

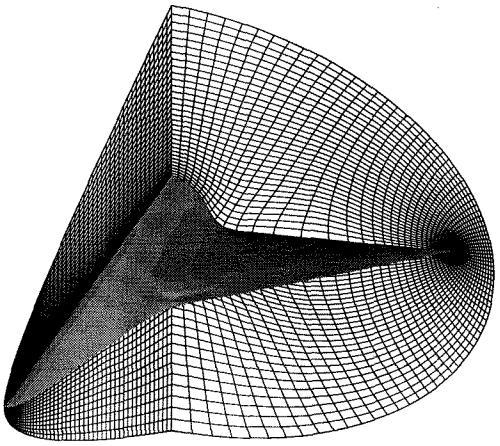

Fig. 2 Fine mesh around the waverider example configuration.

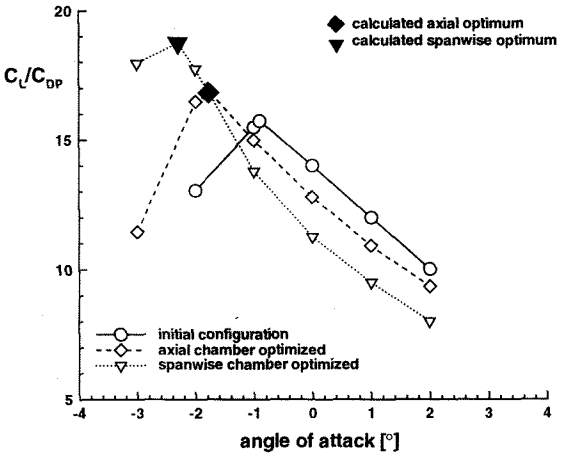

Fig. 3 Lift over drag ratio versus angle of attack for the initial and optimized configurations.

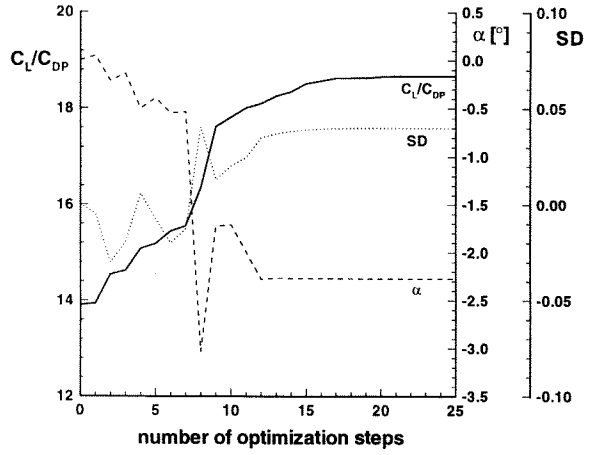

Fig. 4 Optimization history of objective function and both design variables (angle of attack α and spanwise chamber distribution SD) for the waverider example configuration.

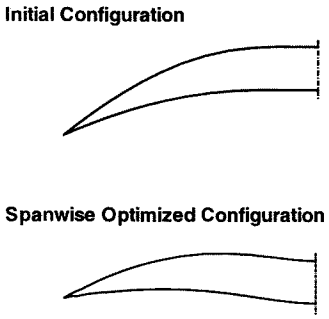

Fig. 5 Comparison of initial and optimized cross sections at ξ' =0.4.

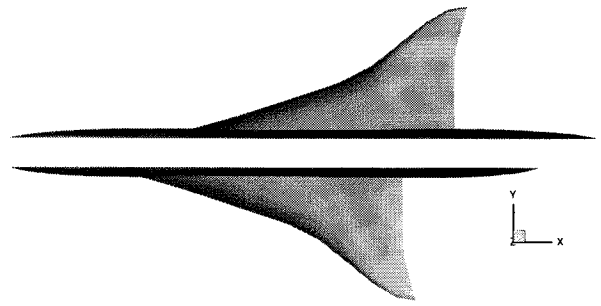

Fig. 6 Planforms resulting from fuselage cone length variations.

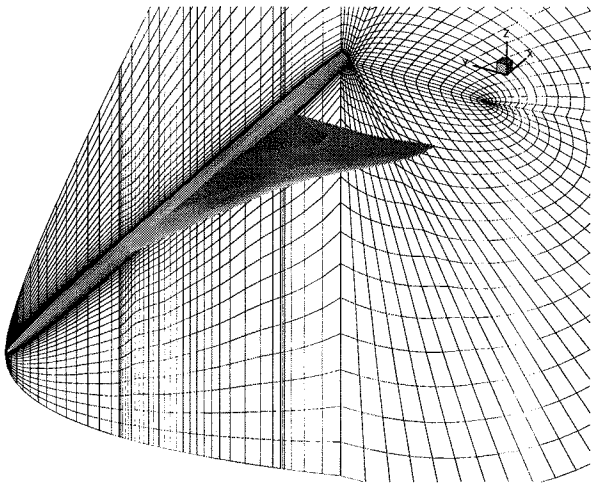

Fig. 7 Medium dense mesh around the generic SCT aircraft (R= 1.75m; cone length= 21m).

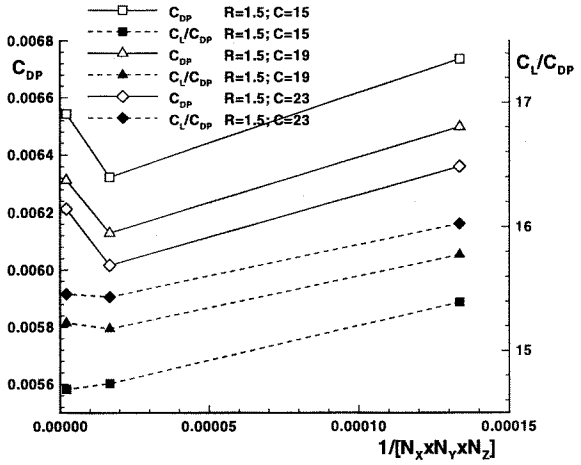

Fig. 8 Dependence of aerodynamic coefficients on different dense meshes.

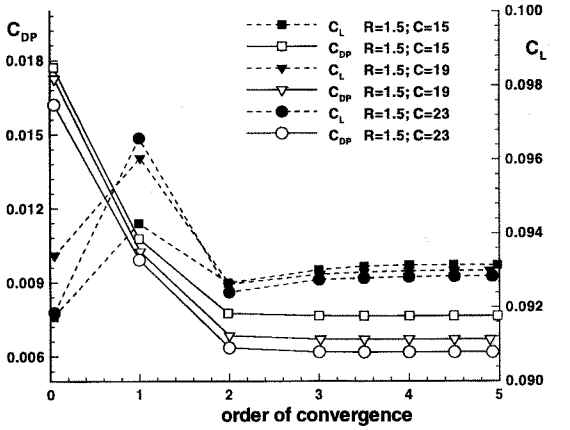

Fig. 9 Convergence of aerodynamic coefficients calculated on the medium dense mesh (48x24x52 cells).

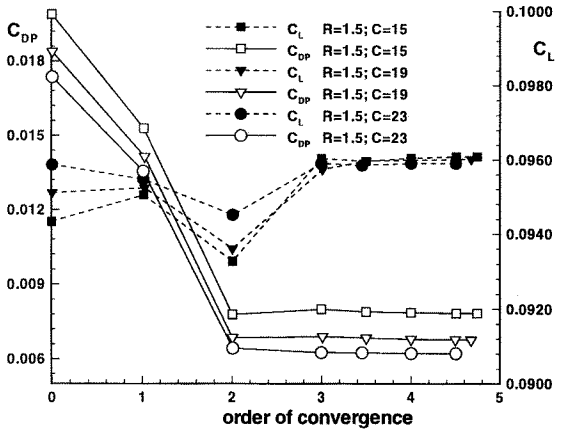

Fig. 10 Convergence of aerodynamic coefficients calculated on the fine mesh (96x48x104 cells).

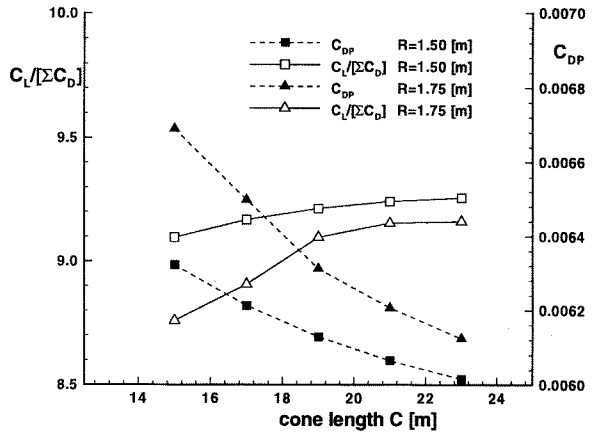

Fig. 11 Lift to drag ratio and pressure drag variation with fuselage cone length for two fuselage radii.

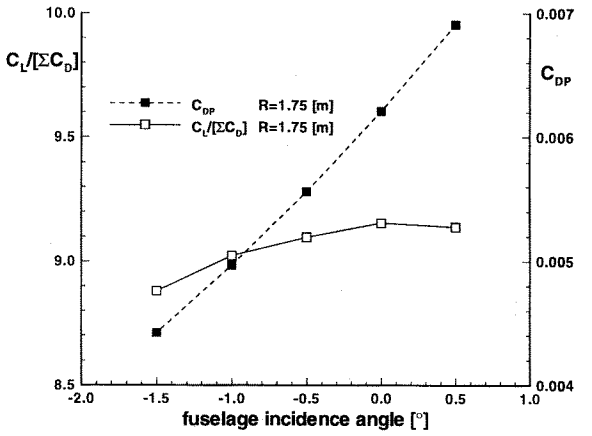

Fig. 12 Lift to drag ratio and pressure drag variation with fuselage (R= 1.75m; C= 21m) incidence.

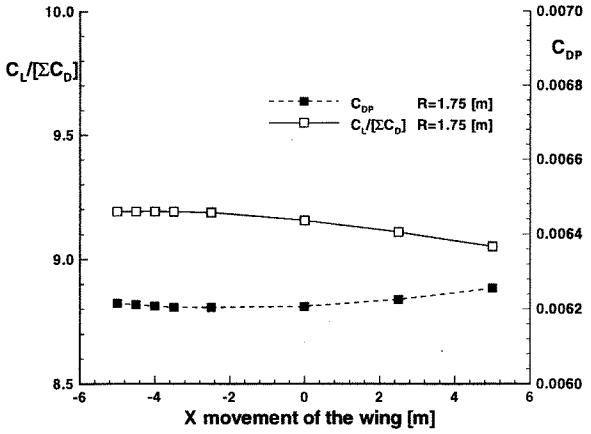

Fig. 13 Lift to drag ratio and pressure drag variation with wing x position relative to the fuselage (R= 1.75m; C= 21m) middle position.

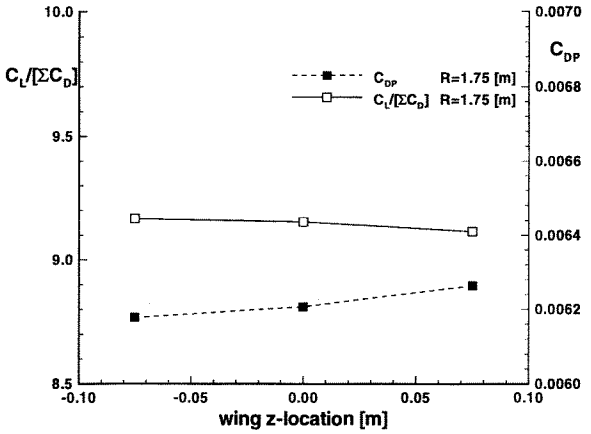

Fig. 14 Lift to drag ratio and pressure drag variation with wing z position relative to the fuselage (R= 1.75m; C= 21m) middle position.

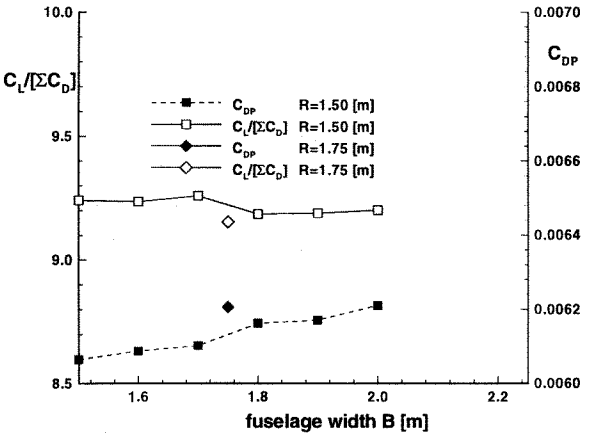

Fig. 15 Lift to drag ratio and pressure drag variation with fuselage (C= 21m) width.